Polymer Chemistry

Accepted Manuscript

ROYAL SOCIETY OF CHEMISTRY

www.rsc.org/polymers

Tumor-targeting delivery of hyaluronic acid-platinum(IV) nanoconjugate to reduce toxicity and improve survival†

Xiang Ling [a], Yan Shen [a], Runing Sun [b], Mengze Zhang [a], Chang Li [a], Jinyin Mao [b], Jing Xing [c], Chunmeng Sun [a, *], Jiasheng Tu [a, *]

[a] State Key Laboratory of Natural Medicines, Department of Pharmaceutics, School of Pharmacy, China Pharmaceutical University, Nanjing 210009, People's Republic of China

[b] Department of Pharmacy, Professional Technology College, China Pharmaceutical University, Nanjing 210009, People's Republic of China

[c] State Key Laboratory of Bioelectronics, Jiangsu Key Laboratory for Biomaterials and Devices, School of Biological Science and Medical Engineering, Southeast University, Nanjing 210096, People's Republic of China

† Electronic Supplementary Information (ESI) available: All the experimental section. Materials, Cell culture and animal use, Synthesis of HA-EDA-Pt(IV) nanoconjugate, Hydrodynamic diameter distribution and zeta potential of HA-EDA and HA-EDA-Pt(IV) nanoconjugate, Typical TEM morphology of (A) HA-EDA and (B) HA-EDA-Pt(IV) nanoconjugate, Release profile of platinum from HA-EDA-Pt(IV) nanoconjugate in vitro, Cytotoxicity evaluation, Confocal laser scanning microscopy analysis for cellular uptake, Determination of platinum contents in the cells, Cell apoptosis, XPS study on the reduction of Pt(IV), Maximum tolerated dose studies in normal mice, Pharmacokinetics studies, Anticancer efficacy evaluation in tumor-bearing mice, Biodistribution of cisplatin and HA-EDA-Pt(IV) nanoconjugate, *In vivo* tumor-targeting observed by Near Infrared Fluorescence (NIRF) imaging.

Abstract:

Cisplatin, albeit bright in clinics, is seriously perplexed by systemic side effects. Consequently, the stimuli-sensitive Pt(IV) pro-drug was synthesized and tethered to ethylenediamine modified hyaluronic acid to form tumor-targeting HA-EDA-Pt(IV) nanoconjugate with reduced adverse reactions and enhanced efficacy. The nanoconjugate with adjustable Pt(IV) segments possessed satisfactory size and potential, exhibited sphericity in shape and released platinum species sustainedly. Cell experiments confirmed that nanoscale conjugates selectively recognized HA receptor, effectively penetrated cell membrane and were finally reduced to active forms with persistent antitumor activity. Toxicological evaluation suggested that the nanomedicine significantly alleviated noxious effects. Alterations of pharmacokinetic profiles and parameters implied *in vivo* behavioral discrepancy after conjugation. Polymer-drug conjugates improved life quality of mice bearing melanoma, prolonged survival, minimized organ toxicity and body weight loss. Favorable tumor-targeting effect was also verified by tissue distribution and *in vivo* imaging analysis. HA-EDA-Pt(IV) nanoconjugate is expected to overcome the bottleneck of present platinum drugs and holds great potential in clinical application for cancer therapy.

Introduction

It has been 169 years since cisplatin was first reported [1]. Some 50 years later, Alfred Werner, won the Nobel Prize in Chemistry, correctly proposed its square planar configuration by his theory of coordination chemistry. As a DNA intercalator, cisplatin has entered into worldwide clinical use due to its broad antitumor activity. Nevertheless, serious side effects including dose limiting nephrotoxicity, neurotoxicity, myelosuppression, anaphylaxis and emetogenicity narrow its major advancements in oncology, another noticeable hurdle covers acquired or intrinsic resistance of tumors [2, 3].

In order to overcome these inherent deficiencies, thousands of platinum complexes have been prepared. Of particular noteworthiness are octahedrally coordinated platinum(IV) with two axial leaving ligands, which could fulfill the mission of cancer curing after reduction [4]. Platinum(IV) retained their + IV valence in blood circulation due to the rapid enzymatic degradation of reducing biomolecules, but could

convert to platinum(II) inside cells where a relatively higher redox potential was always maintained, thereby attaining specific antitumor efficacy with slight side effects. Based on literatures, platinum(IV) with carboxylate ligands have proper reduction potentials (-0.49 V at pH 7.4; -0.42 V at pH 6.0) to manoeuvre antineoplastic activity and seem to be good candidates for platinum-based pro-drugs [5, 6]. Moreover, the carboxylate ligand coordinating with the central platinum ion to weaken its reactivity provides a reactive group to be decorated.

Polymer-drug conjugates that benefit the protection and delivery of platinum(IV) preferentially distribute in cancerous tissue via enhanced permeability and retention (EPR) effect [7, 8]. For instance, when conjugated to amphiphilic tri-block copolymer, platinum(IV) showed reduced systemic toxicity, prolonged blood circulation as well as enhanced antitumor efficacy [9]. Generally, polymer-drug conjugates enter into cancer cells by bulk endocytosis with limited efficacy, while conjugates of tumor interacting moieties and platinum(IV) could further amplify specificity of those pro-drugs [10]. Chitosan nanoparticles, linked with platinum(IV) and vasoactive peptide, had superior efficacy in enhancing drug accumulation in tumors [11]. Mukhopadhyay et al. also successfully improved chemotherapy with platinum(IV)-peptide conjugates by selective drug delivery [12]. Hyaluronic acid (HA), a biodegradable polyanionic polysaccharide, was responsible for receptor-mediated endocytosis, degradation and signal transduction [13]. What's more, CD44, RHAMM, HARE and LYVE-1, which were identified as HA receptor, were found over-expressed on the surface of most malignant cells [14]. In our work, HA was chosen as not only a tumor seeking, but also a biocompatible carrier, so that killed two birds with one stone.

As described in Scheme 1, Cisplatin, written as Pt(II) if necessary, was oxidized with H_2O_2 then reacted with succinic anhydride to form *cis,cis,trans*-dichoro-hydroxyl-succinato-platinum(IV) (abbreviated as Pt(IV) hereafter); meanwhile, HA was modified with ethylenediamine to obtain HA-EDA with rich pendant amino groups. To manufacture HA-EDA-Pt(IV) nanoconjugate, Pt(IV) was linked with HA-EDA via labile succinate amide bonds. Afterwards, a series of evaluation were conducted to characterize physicochemical properties and antitumor efficacy of the nanoconjugate, which could accumulate in tumor location, internalize into carcinoma cells, release Pt(IV) into cytosol for further reduction and induce apoptosis of cancer cells [15, 16].

Results and discussion

Characterization of HA-EDA-Pt(IV) nanoconjugate

As shown in Table S1 †, both HA-EDA and HA-EDA-Pt(IV) nanoconjugate presented nanoscale (~180 nm) with small polydispersity index, while the size of the later slightly increased by reason of loading of Pt(IV), which was consistent with the results from TEM photos (Fig. S1 †) if considering the volume contraction during sample preparation. Furthermore, the conjugation of Pt(IV) to HA-EDA occupied a portion of side amino groups, thereby resulting in decreased zeta potential. Those could also be pieces of evidence for successful conjugation. The drug delivery system, featured as a spherical, nano-size and negatively charged conjugate, possesses great potential to accumulate in tumors at the leaky vasculature.

Platinum release from HA-EDA-Pt(IV) nanoconjugate

Platinum release monitored by Graphite Furnace Atomic Absorption Spectrometry (GFAAS) were carried out at various pH and different concentrations of sodium ascorbate (NaAsc) which were used to simulate the biological environment in blood circulation and cancer cells [17, 18]. As shown in Fig. 1(A), the platinum release rate was significantly higher at pH 5.0 versus pH 7.4, which was presumably because that both HA backbones and linkers between HA and Pt(IV) were easy hydrolyzed under acidic conditions. Typically,

when the platinum loading efficiency was 14.84 w/w%, 80% of the total platinum payloads could be released within 6 h at pH 5.0, while up to 50% after 72 h at pH 7.4, thereby reflecting the pH-sensitive hydrolysis of the nanoconjugate. Moreover, platinum release was also investigated in the presence of NaAsc, which was usually utilized to simulate intracellular and extracellular reductive conditions, that is, ~ 5-10 mM and ~ 27-51 μM, respectively [19, 20]. Unlike Glutathione (GSH) and Dithiothreitol (DTT), NaAsc was able to reduce Pt(IV) but did not further chelate with the reduced Pt(II) [21]. It is believed that Pt(IV), as pro-drugs, are activated extra- or intra-cellularly in vivo by reduction that transforms them to square planar Pt(II) by elimination of axial ligands [22, 23]. As shown in Fig. 1(B), higher concentration of NaAsc led to much faster release of platinum. Besides, a burst release of platinum could also be observed in 5 mM NaAsc group, where 50% of platinum was released within 1 h. The total amount of released platinum, however, was no more than 50% in the case of 0.1 mM NaAsc across the whole release process (up to 72 h). On the one hand, reductive condition plays a crucial role in the release of platinum; on the other hand, it is responsible for the reactivation of Pt(IV) as well. The valence state will be verified in the following section. Compare to normal cells, a much stronger reductive microenvironment in tumor cells was widely reported [24]. Hence, release and reduction for Pt(IV) could primarily take place inside target cells, thereby resulting in lower toxicity to normal tissues. Based on these data, possible release mechanisms of platinum species from the nanoconjugate were depicted in Fig. 1(C). Both acidic and reductive conditions are benefit for the release of platinum. Furthermore, either conjugated or dissociated Pt(IV) could be converted to its active form, Pt(II), by plentiful reducing agents, such as GHS, ascorbic acid, mercaptan, cysteine, metallothioneins (MTs) and etcetera, which exist in carcinoma cells at a higher concentration [25, 26].

Cell proliferation assay

B16-F10, Hep G2 and HEK-293 were exposed to cisplatin and HA-EDA-Pt(IV) nanoconjugate at different doses, they were, 0, 25, 50, 75, 100, 150, 200, 300, 400 mg/L (calculated by cisplatin). HA and carriers were also examined to evaluate the biocompatibility. The relative concentration-response curves were plotted in Fig. 2(1). As it was expected that negligible toxicity to those mammalian cells was observed for HA and HA-EDA across the whole tested concentrations, cisplatin was probably considered the culprit in inducing cell death. Nevertheless, conjugation of Pt(IV) to HA-EDA could greatly decrease its toxicity within 24 h. When the incubation time was extended to 48 h, HA-EDA-Pt(IV) nanoconjugate displayed a comparable cytotoxicity to cisplatin due to sustained hypothesis and reduction inside cells. Thus, the deferred toxicity was supposed to be a nature of HA-EDA-Pt(IV) nanoconjugate which was designed as a pro-drug delivery system and used at a high dose with acceptable adverse reactions [27]. HEK-293 derived from human embryonic kidney cells was selected to evaluate inherent toxicity of platinum complexes. The nanoconjugate decreased the negative impact on cell viability to a certain extent, even 48 h later. It can be concluded that our polymer-drug conjugates could reserve exceptional capacity of cell-killing to target cells and minimize damage to normal cells due to the pro-drug strategy.

Cellular uptake assay

The localization of nanoscale conjugates was visualized by labelling cells with specific fluorescent probes, TRITC, which was conjugated to HA-EDA-Pt(IV) nanoconjugate at a fixed content of 1.03 w/w% to minimize effect on intracellular trafficking. Since cells were thoroughly washed, the fluorescence captured by Confocal Laser Scanning Microscopy (CLSM) was deemed to come from the nanoconjugate taken inside cells. HA-EDA-Pt(IV)-TRITC reflected concentration-dependent uptake in both cell lines, as was

apparent in Fig. 2(2). Besides, incubation for a longer time, *i.e.*, 24 h vs. 4 h, could also receive a higher internalization, suggesting that there was a timing dependency. As is expected, once cells were pre-incubated with HA for 2 h, a dramatic decrease of intracellular fluorescent density would be observed, reflecting that HA should be the substrate involved in the receptor-mediated endocytosis. This result also confirmed our hypothesis: HA-EDA-Pt(IV) nanoconjugate was able to target tumor cells with over-expressed HA receptor [14].

Quantitative assay of internalized platinum

Internalization into tumor cells is the key step before the compounds converting from inactive to active form. Quantitative analysis of platinum transport was a further experiment to confirm the results from CLSM test. In this study, cells incubated with different drugs or combinations at various concentrations were collected at designated time points. All samples were determined and data were given as ng of Pt per mg of protein in Fig. 1(3). Despite of cell lines and platinum drugs, internalization was time- and concentration-dependent, which were consistent with our previous data. Also, addition of HA negatively affected the internalization of HA-EDA-Pt(IV) nanoconjugate, but not cisplatin, reflecting HA and HA-EDA-Pt(IV) were taken up by the same manner. It seems that the transport of polymer-drug conjugates could have more profound effects *in vivo*, going hand in hand with concentration, time and HA receptor. Interestingly, in B16-F10 cells, HA-EDA-Pt(IV) nanoconjugate exhibited a 2 to 4 times higher internalization than cisplatin, while it was less than 2 times for Hep G2 group. The different efficiency in drug delivery was presumably due to the differences in cell membrane permeability and/or HA-receptor expression of these two cell lines.

Programmed cell death

In order to further understand anti-proliferative effect of HA-EDA-Pt(IV) nanoconjugate, cell apoptosis was evaluated and results were presented in Fig. 2(4). HA and HA-EDA were dosed at corresponding concentrations which were equivalent to their contents in nanoconjugate samples. As is expected, carriers showed negligible effect on programmed cell death. Importantly, as the concentration increased from 12.5 to 50 mg/L, cisplatin and HA-EDA-Pt(IV) nanoconjugate exhibited enhanced cell apoptosis in all groups. Furthermore, prolonging incubation time also led to increased apoptotic rates, as dissociation and reduction are necessary steps before Pt(II) works. Furthermore, those thiol-containing biomolecules inside cells, such as GSH and MTs, could also inactivate divalent central Pt atoms via coordination at the initial period [28]. However, with the consumption of reducing biomolecules and high efficiency of cellular uptake, the liberated platinum, *i.e.*, Pt(II), would finally induce permanent cell apoptosis. Pre-incubation with HA lowered cellular uptake amounts of HA-EDA-Pt(IV) nanoconjugate in the first 24h, thereby leading to slightly decreased apoptotic rate. However, as the incubation time went on, the dissociation between HA and HA receptors would be benefit for the internalization of HA-EDA-Pt(IV) nanoconjugate and further cell apoptosis [29]. With the help of receptor-mediated internalization, positive shift of reduction potential in cytoplasm and acidic environment in endosome compartments, the recuperative Pt(II) species could bind to purine and pyrimidine bases, cause crosslinking of DNA, interfere with cell division by mitosis. The damaged DNA elicits DNA repair mechanisms, which ultimately activate programmed cell death when repair seems impossible.

Oxidation state of platinum species in vitro

GFAAS could measure the total platinum amount precisely but not provided further information about

those precursors, even the valence state. Thus, XPS might be an effective complement to reveal oxidation state of platinum species [9]. As platinum with different valence states possessed different binding energies, the parameters, *i.e.*, $Pt_{4f(5/2)}$ and $Pt_{4f(7/2)}$, should be helpful for us to figure out the distribution of valence states of platinum under different conditions. In this study, the binding energy-arbitrary counts curves were shown in Fig. 3 and related data were collected in Table 1 in detail. Typically, the Pt_{4f} would shift to high binding energy as the valence state converted from + II valence, *i.e.*, cisplatin, to + IV valence, *i.e.*, *cis,cis,trans*-$[Pt(NH_3)_2Cl_2(OH)_2]$, Pt(IV) and HA-EDA-Pt(IV) nanoconjugate, and vice versus. Illatively, co-existence of Pt(II) and Pt(IV) should give four peaks. However, the nearly identical binding energy resulted in an overlap of the peaks of $Pt(II)_{4f(5/2)}$ of $Pt(IV)_{4f(7/2)}$, thus, as shown in Fig. 3(e, f, g, h), it could be concluded that a portion of Pt(IV) were converted to Pt(II) after treatment with GSH, NaAsc, B16-F10 and Hep G2 for 24 h. However, two peaks of + IV valence forms in Fig. 3(i) showed up to 24-hour stability of HA-EDA-Pt(IV) nanoconjugate in plasma, further confirming the necessity of reductive condition, such as microenvironment in tumor tissues, for drug release and valence state conversion. In comparison to normal tissues, reductive and hypoxic microconditions were considered as the major characteristics of carcinoma tissues, which were greatly benefit for the constant conversion of Pt(IV) to Pt(II) with plentiful reducing biomolecules. Moreover, the difference in reduction potential between the intracellular and extracellular milieu could contribute to redox-sensitive drug release and render HA-EDA-Pt(IV) nanoconjugate promising for tumor-specific drug delivery.

Evaluation of maximum tolerated dose (MTD)

ICR mice were treated with gradient doses of platinum drugs to explore MTD, and their body weight change and survival state were recorded in Fig. 4. Mice administrated with 8.00 mg/kg cisplatin suffered immense weight loss (> 20%), and death cases could be found in the higher dose group (14.220 mg/kg), which were consistent with previous studies [30]. For the nanomedicine, obvious weight loss could be observed in the two highest dose groups (814.979 and 1086.639 mg/kg), which unexpectedly started to regain weights soon and reached their initial weights on day 9, and dose of 1086.639 mg/kg caused mice death. Based on these data, 611.234 mg/kg was regarded as the MTD of HA-EDA-Pt(IV) nanoconjugate, which was more than 30 fold (calculated by cisplatin) higher than that of cisplatin. Dose intensification of cisplatin in clinical seems meaningful as it may allow patients to receive higher doses of chemotherapeutics without severe systemic side effects.

Pharmacokinetics

Pharmacokinetic profiles were investigated between cisplatin and HA-EDA-Pt(IV) nanoconjugate, and data were analyzed using a Phoenix WinNonlin 6.3 Program. The results suggested that both drugs followed a two-compartment pharmacokinetic model, based on the residual sum of squares and minimum Akaike's information criterion (AIC) value. What's more, non-compartment model was also applied to analyze change of pharmacokinetic behaviors. The plasma platinum concentration-time profiles were illustrated in Fig. 5. Although rapid elimination of platinum from blood circulation occurred both for cisplatin and HA-EDA-Pt(IV) nanoconjugate, curves of these preparations were apparently different in concentration and significantly delayed release was found in polymer-drug conjugates group. HA-EDA-Pt(IV) nanoconjugate had a longer blood retention as compared with unconjugated cisplatin. $AUC_{0\rightarrow inf}$ and $MRT_{0\rightarrow inf}$ of our nanoconjugate were greatly higher than those in cisplatin group, *i.e.*, 5- and 1.8-fold, respectively, indicating an obvious retardation in clearance. Extended blood circulation time would greatly promote accumulation in tumors through EPR effect. Furthermore, CL and V_{ss} decreased by

82% and 60% in the nanoconjugate group versus cisplatin group. These results could be attributable to slight biodistribution of the nanomedicine in normal tissues as well as retention in blood circulation. Based on traditional compartmental model, A and B increased by 1.4- and 3-fold, while both α and β decreased to ~50% for HA-EDA-Pt(IV) nanoconjugate versus cisplatin. By contrast, the nanomedicine approximately doubled both $t_{1/2\alpha}$ and $t_{1/2\beta}$, which were consistent with the sustained-release nature of polymer-drug conjugates. After intravenously injecting the nanoconjugate, k_{10} quartered, k_{12} went down by 1.8 time, and k_{21} maintained at the same level, compared with cisplatin. Taking the negatively charged surface and nanoscale size of polymer-drug conjugates, it should prefer to stay in central compartment with prolonged retention time. HA-EDA-Pt(IV) nanoconjugate with longer circulation time could significantly ameliorate *in vivo* pharmacokinetics of cisplatin. We could draw a conclusion that bioavailability of the nanomedicine would dramatically increase.

***In vivo* antitumor efficacy**

Owing to specific internalization pathway, enhanced tolerability, and prolonged circulation, HA-EDA-Pt(IV) nanoconjugate might conduce to better antitumor efficacy with reduced systemic toxicity. In this section, *in vivo* experiments were performed systematically in tumor-bearing mice. To evaluate nephrotoxicity, the concentrations of two biomarkers, BUN and Scr, were measured. What's more, alterations of hepatic function indexes (ALT, AST, ALP) were also checked. Data were collected in Table. 3. Mice treated with cisplatin displayed higher levels of all these parameters, especially BUN and Scr. Considering slight increases of ALT, AST and ALP, liver function was also influenced to some degree. These results indicate that cisplatin is much toxic and the challenge to employ it safely is to design an appropriate drug delivery system. Mice treated with HA-EDA-Pt(IV) nanoconjugate had moderate alterations of ALP and Scr and down regulation of ALT, AST and BUN. Anyhow, these parameter levels were comparable to those in control groups, *i.e.*, physiological saline and HA-EDA, demonstrating that it's hard to induce severe adverse reactions after multiple dose administration of the nanoconjugate.

HA-EDA showed no effects on tumor inhibition. Inhibition rate of cisplatin group was higher (42.19%), but there was a very significant increase in HA-EDA-Pt(IV) nanoconjugate group (69.38%, $p < 0.01$). From above evaluation, the nanomedicine displayed the best antineoplastic capability among all groups. As shown in Fig. 6(1), there was no difference in tumor sizes from mice receiving physiological saline or HA-EDA. In contrast, tumor growth could be well restrained in mice undergoing platinum drugs, despite cisplatin or HA-EDA-Pt(IV) nanoconjugate, while the restraint effect of the later was much greater.

For safety consideration, the toxicity of multiple dose administration was also investigated by monitoring the weight change of major organs. There was no difference in the cases of lung and brain, while significant difference was found in the weight change of heart, liver, spleen and kidney in Fig. 6(2). Seemingly, long-term toxicity of parent drug, cisplatin, was serious for above organs. The reduced tumor weights also validated enhanced inhibition efficacy of the nanoconjugate (0.3654 ± 0.0932 g) towards cisplatin (0.6897 ± 0.1166 g). Statistical analysis could prove that those tumors treated with the nanomedicine are significantly smaller than others, implying that polymer-drug conjugates induce an effective antitumor response *in vivo*.

To further evaluate organ toxicity, solid tissues were embedded in paraffin and stained with hematoxylin and eosin (HE). As shown in Fig. 6(3), pathological analysis gave evidence of no morphological change of heart and brain in all groups, even though the weight change of heart was significant. However, varying degrees of damage to other organs, including liver, spleen, lung and kidney,

was accompanied with those receiving long-term injection of platinum drugs. Cisplatin group displayed noticeable signals of damage to liver, with slight vacuolar degeneration. In contrast, treatment of mice with the nanoconjugate obviously reduced the blight of liver. The structure of spleen was incomplete, white pulp diminished and shrank, and the number of lymphocytes decreased sharply in the mice receiving cisplatin, while those receiving the nanoconjugate exhibited alleviated symptoms. Atrophy of most areas of lung at the early phase and alveolar collapse were observed in cisplatin group. Nevertheless, no obvious pathological change of lung was founded in other three groups. The most important thing was that free cisplatin at therapeutic dose induced severe nephrotoxicity, such as edema and even ballooning degeneration of renal tubular epithelial cells from deep cortical layer to renal medulla, an increase in cell size, cytoplasmic relaxation, exudates from glomerular capsule, much smaller glomeruli of kidney. Whereas, the nephrotoxicity was effectively avoided in nanomedicine group, suggesting that HA-EDA-Pt(IV) nanoconjugate was better for long-term administration.

On the premise of safety, reliable efficacy became a major concern for *in vivo* application of chemotherapeutics. In Fig. 6(3), tumor cells owning large nucleuses and spherical or spindle shapes were captured in physiological saline and HA-EDA groups, where more chromatin and binucleolates were also visualized, revealing a rapid tumor proliferation. As estimated by average cell numbers in each microscopic field of platinum drug groups, *i.e.*, cisplatin and polymer-drug conjugates, the tumor cellularity was found significant declines, which was consistent with tissue necrosis, extensive cell shrinkage and fragmentation. Nuclear chromatin was concentrated and distributed around the edge, and many nuclei became pyknotic and had undergone karyorrhexis or/and karyolysis. Most importantly, HA-EDA-Pt(IV) nanoconjugate group exhibited the largest necrosis area among all groups.

The mild pathological change of major organs and critical necrosis of tumors would be the huge vindication of the nanomedicine's curative effect. To explore the mechanism of antineoplastic activity of HA-EDA-Pt(IV) nanoconjugate, tumor apoptosis was further investigated. The tumor protein p53, which was able to activate a series of DNA repair proteins when DNA had sustained damage, was analyzed by immunohistochemistry [31]. Compared with cisplatin, p53 protein increased intensively after treatment with HA-EDA-Pt(IV) nanoconjugate, emphasizing the greater efficacy of the nanomedicine. Moreover, as detected by TUNEL, tumor tissues from platinum drug groups, *i.e.*, cisplatin and HA-EDA-Pt(IV) nanoconjugate, had extensive regions of apoptotic cells, especially the ones administrated with nano-formulation, whereas such apoptotic cells were less presented in the other two groups, *i.e.*, saline and HA-EDA. These data were consistent with microscopic examination. It could be demonstrated that polymer-drug conjugates efficiently deliver bioactive drugs to tumor sites, leading to reduced cell proliferation, increased apoptosis and then a persistent inhibition on tumor growth.

Fig. 6(4) reflected the efficacy of platinum drugs, *i.e.*, cisplatin and nanoscale conjugates, in prolonging the survival time of tumor-bearing mice obviously, while the later did much better. Unfortunately, 100% animal death occurred at the first day of third week after initiating treatment of cisplatin due to self-toxicity, all mice without receiving platinum died with two weeks. In contrast, the nanomedicine treated animals could live for up to four weeks.

The relative tumor volumes were also recorded in Fig. 6(5) and the significantly reduced tumor volumes demonstrated expectant inhibition efficacy of the nanomedicine. The average tumor sizes of control groups were approximately 500-1300 mm^3 two weeks later, conforming that carriers couldn't alter the natural progression of melanoma. Animals treated with multidose of cisplatin developed tumors with size of 850 mm^3 on average after two weeks. By comparison, HA-EDA-Pt(IV) nanoconjugate treated mice reached an average tumor size of 360 mm^3 four weeks later, suggesting that their tumors grew in a

decelerated mode. Thus, platinum species released from nanoscale conjugates could enhance effect and prolong survival time, achieve much better clinical evaluation than conventional cisplatin.

What's more, the change in body weight was also collected as an indication of drug safety and depicted in Fig. 6(6). Mice receiving cisplatin were very anorectic and exhibited significant weight loss, whereas those treated with the nanoconjugate had the contrasting growth, implying fewer side effects. There was little change in weight of control groups. For improvement in symptoms and putting on weight during chemotherapy, polymer-drug conjugates would be the better choice.

Biodistribution of platinum in plasma and organs

A notable advantage of the nanoconjugate was the possibility to alter tissue distribution of platinum complexes which might benefit the accumulation in tumor sites. The mice were sacrificed at defined time points and total platinum content, which stood for the nanoconjugate content based on the assumption that HA-EDA-Pt(IV) nanoconjugate kept intact before entering tissues, was measured. Several features could be summarized from Fig. 7. The platinum concentration in both organs and plasma showed successive decrease with time. Originally, cisplatin was mainly partitioned in kidney, secondly in liver, then lung, heart, spleen and brain, which demonstrated rapid clearance and explained high nephrotoxicity. After administration of HA-EDA-Pt(IV) nanoconjugate, similar patterns were also observed, but with reduced platinum content in most organs at each time point, especially in kidney. These would benefit enhancement of bioavailability and alleviation of damage to organs. As for plasma, platinum concentration was significantly improved after conjugation. Even 24 hours later, the platinum content was still as high as 5 times, compared to cisplatin, implying prolonged circulation and possible enrichment in tumors. Obviously, the nanoconjugate would be protected against the attack of reticuloendothelial system, reduce liver metabolism and renal excretion, and increase the residence time in blood. From biodistribution assay, a rational conclusion could be drawn that the nanoconjugate has a relatively longer systemic circulation time, therefore provides enough time to accumulate in tumor vasculature by passive-targeting in nature due to EPR effect [32].

Site-specific delivery of Cy7, SE-labeled nanoconjugate to melanoma-bearing mice

As our nanoconjugate was engineered for tumor-specific delivery of Pt(IV), herein, after labelling with a fluorescent dye, Cy7, SE, HA-EDA-Pt(IV)-Cy7, SE was injected into melanoma-bearing C57BL/6J mice for biodistribution study. Notwithstanding the conjugation efficiency of Cy7, SE was 3.05%, the fluorescent intensity was strong enough to trace the kinetics of HA-EDA-Pt(IV)-Cy7, SE *in vivo*. Moreover, poor dye loading efficiency minimized its effect on peak time and elimination rate of HA-EDA-Pt(IV) nanoconjugate. A tendency of signal intensity change was observed by real-time imaging. As shown in Fig. 8(1), the free dye exhibited a completely different kinetic behavior compared with HA-EDA-Pt(IV)-Cy7, SE, suggesting that the conjugation of Cy7, SE was stable for *in vivo* distribution study and that the strong fluorescent signal in tumor sites was unlikely resulting from the property of the dye itself. It could be explained that the defects of neovasculature result in continuous leak of HA-EDA-Pt(IV)-Cy7, SE. On the other hand, those large molecules are entrapped in tumor interstitium owing to the slow venous return and poor lymphatic clearance [33]. In addition, the *ex vivo* images of isolated tissues indicated that the tumor retention of HA-EDA-Pt(IV)-Cy7, SE could be detected for more than 12h. Surprisingly, a strong fluorescent signal could also be found from the plasma in the nanoconjugate group, suggesting the great stability of HA-EDA-Pt(IV) nanoconjugate *in vivo*. Besides, a long retention time in plasma was also benefit for the targeting delivery of platinum and achieving

sustained chemotherapy.

Additionally, tissues were sectioned to further validate *in vivo* targeting effect. Much lower fluorescent signals in lung and kidney were captured in Fig. 8(2) as compared to Cy7, SE group, while no significant difference was detected in heart, liver, spleen and brain between groups. Importantly, the level of free Cy7, SE was greatly increased in kidney, likely due to the clearance of the dye from the body. However, as for tumors, sample from nanoconjugate group displayed much stronger fluorescent signals than that from free dye group, which was greatly consistent with the *in vivo* imaging results. Hence, a favorable distribution for HA-EDA-Pt(IV)-Cy7, SE with distinctly increased accumulation in tumors could be proved. Unlike non-specific delivery of Cy7, SE, the process of partitioning, in addition to metabolism and excretion, could be considered as targeting effect.

Conclusions

To sum up, a platinum-based pro-drug was constructed and linked to biodegradable HA to obtain HA-EDA-Pt(IV) nanoconjugate. The nanoconjugate was designed to achieve tumor-specific therapy via multi steps, such as receptor-mediated endocytosis as well as microenvironment-based drug release and reactivation. The appropriate physicochemical properties and *in vivo* data support our prospect that the nanoconjugate could deliver Pt(IV) to tumor tissues and cells, where Pt(IV) could be converted into its active form, Pt(II), thereby curing cancer and minimizing side effects. Briefly, the nano-sized delivery system provides a unique strategy for transport of other platinum complexes.

Acknowledgements

This research was financially supported by the National Natural Science Foundation of China for Young Scholar (NO. 81201182), the Fundamental Research Funds for the Central Universities for Cultivation Project (NO. JKPZ2013006) and the Doctoral Fund of Ministry of Education of China for Youth Scholars (NO. 20130096120003). The authors also acknowledge Jianzhao Wang, Jiarong Xie, Yipeng Su and Dr. Yang Chen for their kind assistance in experimental operation and data processing.

Notes and references

1 M. Peyrone, *Annalen der Chemie und Pharmacie*, 1844, 51, 1-29.

2 S. Dasari and P. B. Tchounwou, *Eur. J. Pharmacol.*, 2014, 740, 364-378.

3 M. Kartalou and J. M. Essigmann, *Mutat. Res.*, 2001, 478, 23-43.

4 H. S. Oberoi, N. V. Nukolova, A. V. Kabanov and T. K. Bronich, *Adv Drug Deliv Rev*, 2013, 65, 1667-1685.

5 M. D. Hall, H. R. Mellor, R. Callaghan and T. W. Hambley, *J. Med. Chem.*, 2007, 50, 3403-3411.

6 S. Dhar, W. L. Daniel, D. A. Giljohann, C. A. Mirkin and S. J. Lippard, *J. Am. Chem. Soc.*, 2009, 131, 14652-14653.

7 M. R. Dreher, W. Liu, C. R. Michelich, M. W. Dewhirst, F. Yuan and A. Chilkoti, *J. Natl. Cancer Inst.*, 2006, 98, 335-344.

8 A. I. Minchinton and I. F. Tannock, *Nat. Rev. Cancer*, 2006, 6, 583-592.

9 H. Xiao, H. Song, Y. Zhang, R. Qi, R. Wang, Z. Xie, Y. Huang, Y. Li, Y. Wu and X. Jing, *Biomaterials*, 2012, 33, 8657-8669.

10 J. D. Byrne, T. Betancourt and L. Brannon-Peppas, *Adv Drug Deliv Rev*, 2008, 60, 1615-1626.

11 X. Wang, C. Yang, Y. Zhang, X. Zhen, W. Wu and X. Jiang, *Biomaterials*, 2014, 35, 6439-6453.

12 S. Mukhopadhyay, C. M. Barnes, A. Haskel, S. M. Short, K. R. Barnes and S. J. Lippard, *Bioconjug*

Chem, 2008, 19, 39-49.

13 Y. Shen, Q. Li, J. S. Tu and J. B. Zhu, *Carbohydrate Polymers*, 2009, 77, 95-104.

14 V. M. Platt and F. C. Szoka, Jr., *Mol Pharm*, 2008, 5, 474-486.

15 K. Y. Choi, G. Saravanakumar, J. H. Park and K. Park, *Colloids Surf. B Biointerfaces*, 2012, 99, 82-94.

16 S. Aryal, C. M. Hu and L. Zhang, *ACS Nano*, 2010, 4, 251-258.

17 H. T. Duong, V. T. Huynh, P. de Souza and M. H. Stenzel, *Biomacromolecules*, 2010, 11, 2290-2299.

18 S. Choi, C. Filotto, M. Bisanzo, S. Delaney, D. Lagasee, J. L. Whitworth, A. Jusko, C. R. Li, N. A. Wood, J. Willingham, A. Schwenker and K. Spaulding, *Inorg. Chem.*, 1998, 37, 2500-2504.

19 P. Washko, D. Rotrosen and M. Levine, *Am. J. Clin. Nutr.*, 1991, 54, 1221S-1227S.

20 H. Reiber, M. Ruff and M. Uhr, *Clin. Chim. Acta*, 1993, 217, 163-173.

21 K. Lemma, A. M. Sargeson and L. I. Elding, *J Chem Soc Dalton*, 2000, DOI: Doi 10.1039/A909484i, 1167-1172.

22 E. Wexselblatt and D. Gibson, *J. Inorg. Biochem.*, 2012, 117, 220-229.

23 M. D. Hall and T. W. Hambley, *Coord. Chem. Rev.*, 2002, 232, 49-67.

24 P. Kuppusamy, H. Li, G. Ilangovan, A. J. Cardounel, J. L. Zweier, K. Yamada, M. C. Krishna and J. B. Mitchell, *Cancer Res.*, 2002, 62, 307-312.

25 F. Meng, W. E. Hennink and Z. Zhong, *Biomaterials*, 2009, 30, 2180-2198.

26 S. Dhar, F. X. Gu, R. Langer, O. C. Farokhzad and S. J. Lippard, *Proc Natl Acad Sci U S A*, 2008, 105, 17356-17361.

27 M. J. Ferguson, F. Y. Ahmed and J. Cassidy, *Drug Resist. Updat.*, 2001, 4, 225-232.

28 M. Ohmichi, J. Hayakawa, K. Tasaka, H. Kurachi and Y. Murata, *Trends Pharmacol. Sci.*, 2005, 26, 113-116.

29 L. A. Sklar, D. A. Finney, Z. G. Oades, A. J. Jesaitis, R. G. Painter and C. G. Cochrane, *J. Biol. Chem.*, 1984, 259, 5661-5669.

30 Y. Xiong, W. Jiang, Y. Shen, H. Li, C. Sun, A. Ouahab and J. Tu, *Biomaterials*, 2012, 33, 7182-7193.

31 S. Sengupta and C. C. Harris, *Nat. Rev. Mol. Cell Biol.*, 2005, 6, 44-55.

32 A. K. Iyer, G. Khaled, J. Fang and H. Maeda, *Drug Discov. Today*, 2006, 11, 812-818.

33 S. Jaracz, J. Chen, L. V. Kuznetsova and I. Ojima, *Bioorg. Med. Chem.*, 2005, 13, 5043-5054.

Table 1 Valence state analyses of Pt in various samples by XPS.

Number	Sample name	Binding energy (ev)		Oxidation state of Pt
		$Pt_{4f(7/2)}$	$Pt_{4f(5/2)}$	
a	Cisplatin	72.50	75.87	+2
b	*Cis,cis,trans*-$[Pt(NH_3)_2Cl_2(OH)_2]$	75.29	78.64	+4
c	Pt(IV)	75.34	78.65	+4
d	HA-EDA-Pt(IV) nanoconjugate	74.37	77.47	+4
e	HA-EDA-Pt(IV) nanoconjugate + GSH	71.92; 75.02; 78.18		+2, +4
f	HA-EDA-Pt(IV) nanoconjugate + NaAsc	72.52; 75.51; 78.39		+2, +4
g	HA-EDA-Pt(IV) nanoconjugate + B16-F10	72.33; 75.66; 78.45		+2, +4
h	HA-EDA-Pt(IV) nanoconjugate + Hep G2	71.98; 75.13; 78.36		+2, +4
i	HA-EDA-Pt(IV) nanoconjugate + rat plasma	75.68	78.99	+4

Table 2 Pharmacokinetic parameters of cisplatin and HA-EDA-Pt(IV) nanoconjugate post a single intravenous injection to half male and half female rats. Data were presented as means ± SD, n = 12.

Model type	Parameter	Unit	Cisplatin	HA-EDA-Pt(IV) nanoconjugate
Non-compartment model	$AUC_{0\rightarrow inf}$	(h·mg)/L	27.515 ± 1.187	143.395 ± 2.172
	CL	L/(h·kg)	0.327 ± 0.149	0.057 ± 0.010
	V_{ss}	L/kg	7.432 ± 1.348	2.777 ± 0.365
	$MRT_{0\rightarrow inf}$	h	26.531 ± 1.461	49.811 ± 1.056
Two-compartment model	A	mg/L	16.680 ± 1.898	22.738 ± 0.717
	α	1/h	4.329 ± 0.585	2.271 ± 0.160
	B	mg/L	0.887 ± 0.148	2.726 ± 0.066
	β	1/h	0.054 ± 0.018	0.026 ± 0.001
	$t_{1/2\alpha}$	h	0.162 ± 0.024	0.306 ± 0.022
	$t_{1/2\beta}$	h	13.656 ± 3.868	26.441 ± 0.961
	k_{10}	h^{-1}	0.901 ± 0441	0.224 ± 0.016
	k_{12}	h^{-1}	3.213 ± 0.396	1.807 ± 0.141
	k_{21}	h^{-1}	0.269 ± 0.023	0.266 ± 0.009

Table 3 Variations of the indexes (ALT, AST, ALP, BUN and Scr concentration) in B16-F10-bearing C57BL/6J mice administrated with different chemotherapeutics.

Group drug	ALT (IU/L)	AST (IU/L)	ALP (IU/L)	BUN (mmol/L)	Scr (μmol/L)
Physiological saline	106.00 ± 2.71	902.71 ± 5.28	75.00 ± 2.89	10.34 ± 1.43	9.86 ± 1.68
Cisplatin	126.75 ± 4.99	1006.50 ± 9.29	161.75 ± 8.26	27.93 ± 0.51	40.75 ± 2.06
HA-EDA	102.14 ± 4.34	912.57 ± 4.24	60.14 ± 3.13	7.84 ± 0.92	12.71 ± 2.43
HA-EDA-Pt(IV) nanoconjugate	102.33 ± 3.72	856.33 ± 7.94	87.67 ± 4.93	8.42 ± 0.92	14.00 ± 2.5

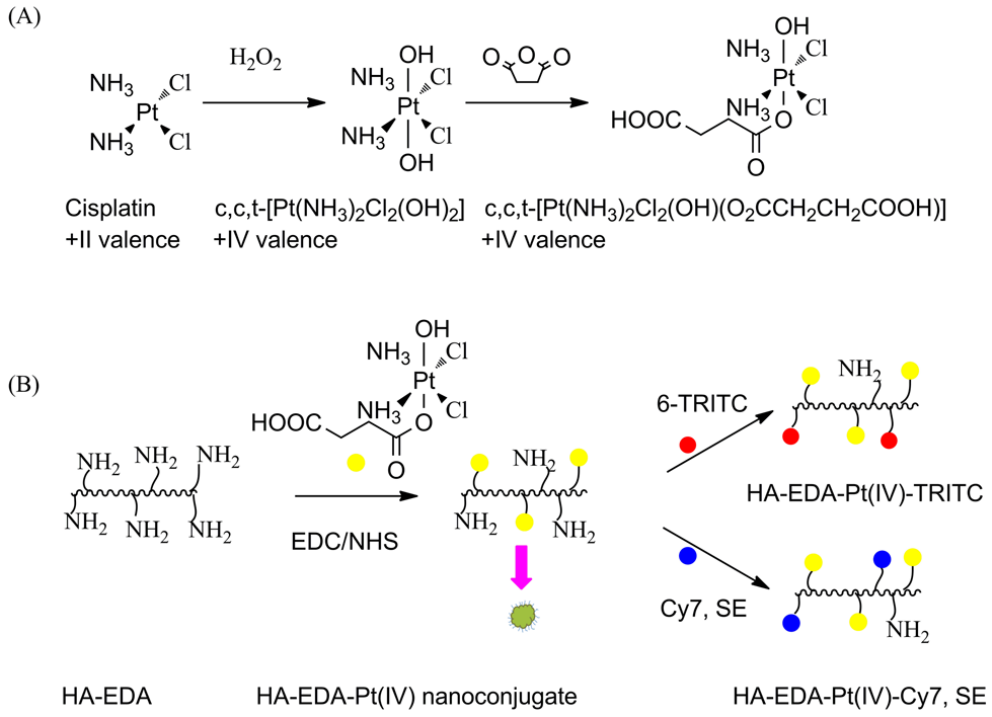

Scheme 1 Synthetic routes of (A) Pt(IV); (B) HA-EDA-Pt(IV) nanoconjugate, HA-EDA-Pt(IV)-TRITC and HA-EDA-Pt(IV)-Cy7, SE.

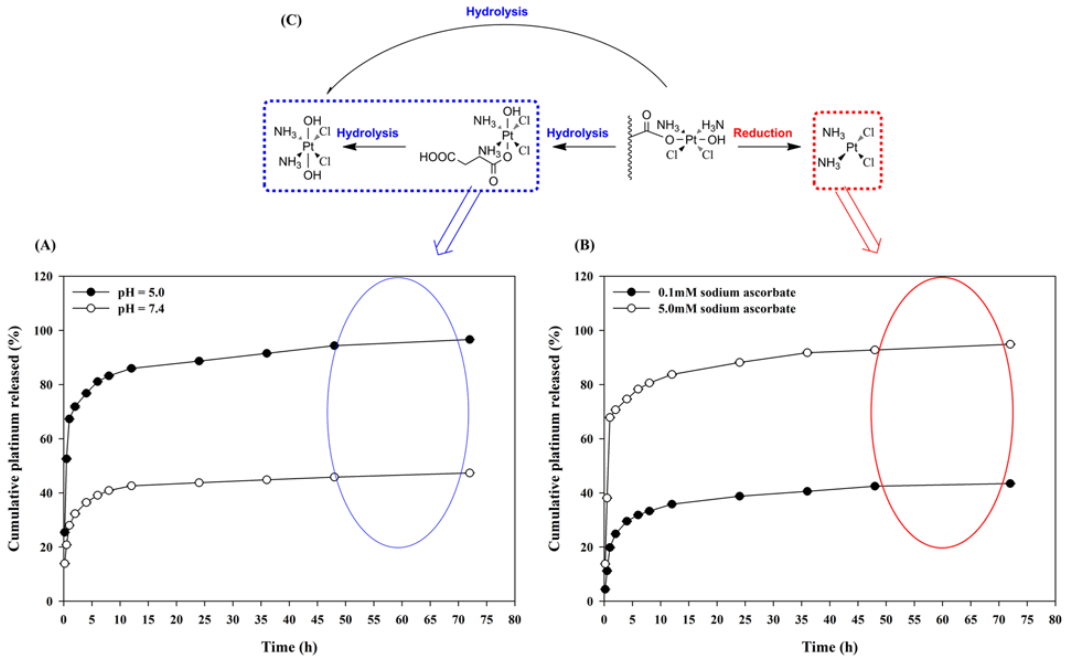

Fig. 1 Platinum release profiles from HA-EDA-Pt(IV) nanoconjugate: (A) in buffer solutions at pH 5.0 and 7.4; (B) in 0.1 and 5 mM NaAsc aqueous solutions. (C) Possible release routes of platinum species based on hydrolysis and reduction. The cumulative percentage of released platinum to total payloads in the nanoconjugate was plotted as a function of time.

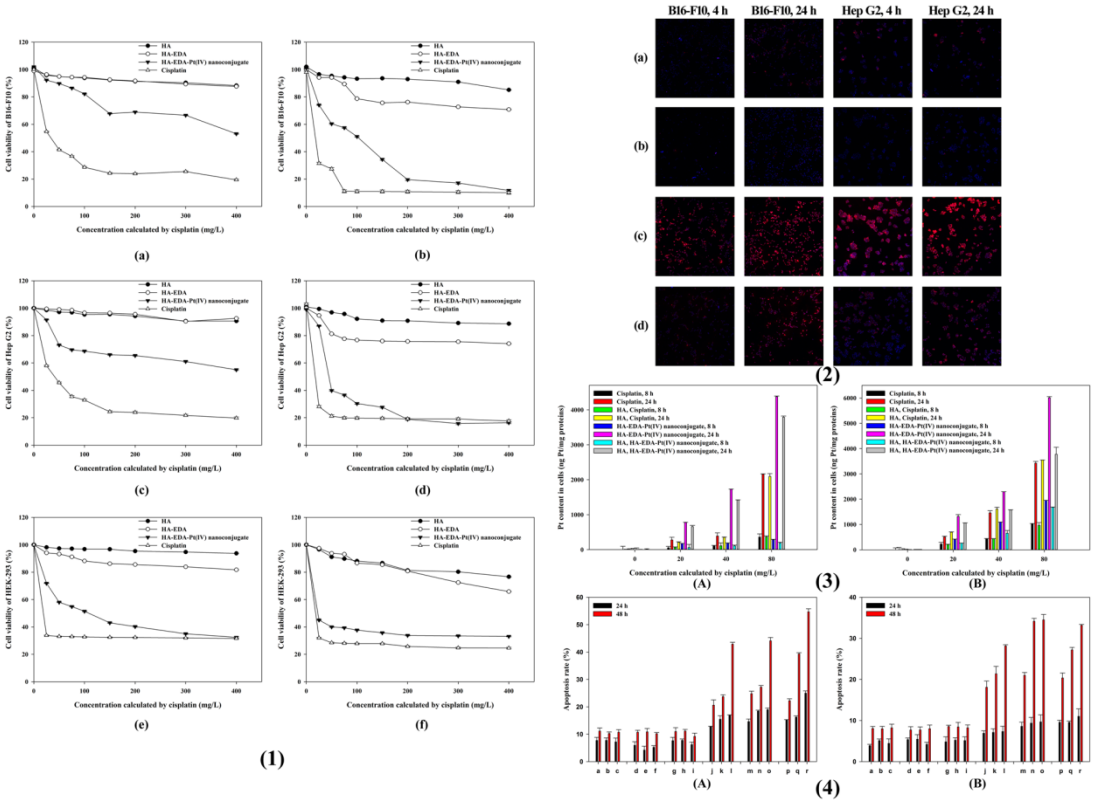

Fig. 2 (1) In vitro cytotoxicity of HA, HA-EDA, HA-EDA-Pt(IV) nanoconjugate and cisplatin against B16-F10, Hep G2 and HEK-293 at (a, c, e) 24 and (b, d, f) 48 h; (2) Tumor cells were incubated with (a, b) 5 and (c, d) 50 mg/L HA-EDA-Pt(IV)-TRITC (red). (b, d) Receptor competition study was also conducted with excess of HA. The nuclei were stained by DAPI (blue); (3) Cellular uptake of cisplatin and HA-EDA-Pt(IV) nanoconjugate at 8 and 24 h determined by GFAAS. (A) B16-F10 and (B) Hep G2 were incubated in the present of platinum drugs at equivalent cisplatin concentrations; (4) Flow cytometric analysis for apoptosis in (A) B16-F10 and (B) Hep G2 following treatment with platinum drugs. The formulations were listed as follows: (a, b, c) blank control, (d, e, f) HA, (g, h, i) HA-EDA, (j, k, l) Excess HA was added to cells 2 h before incubation with the nanomedicine at various levels, (m, n, o) HA-EDA-Pt(IV) nanoconjugate at equivalent cisplatin concentrations, (p, q, r) cisplatin at doses of 12.5, 25 and 50 mg/L.

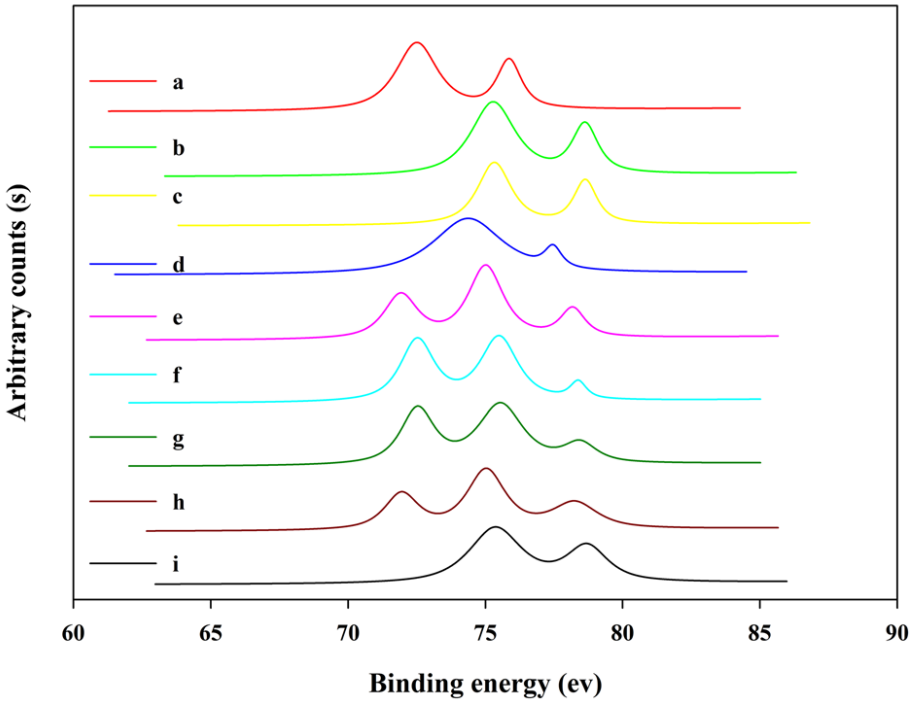

Fig. 3 X-ray photoelectron spectroscopic (XPS) study of Pt_{4f} on (a) cisplatin, (b) *cis*,*cis*,*trans*-$[Pt(NH_3)_2Cl_2(OH)_2]$, (c) Pt(IV), (d) HA-EDA-Pt(IV) nanoconjugate, as well as the co-incubation products of HA-EDA-Pt(IV) nanoconjugate with (e) 6 mM GSH, (f) 3 mM NaAsc, (g) B16-F10, (h) Hep G2 and (i) rat plasma, respectively.

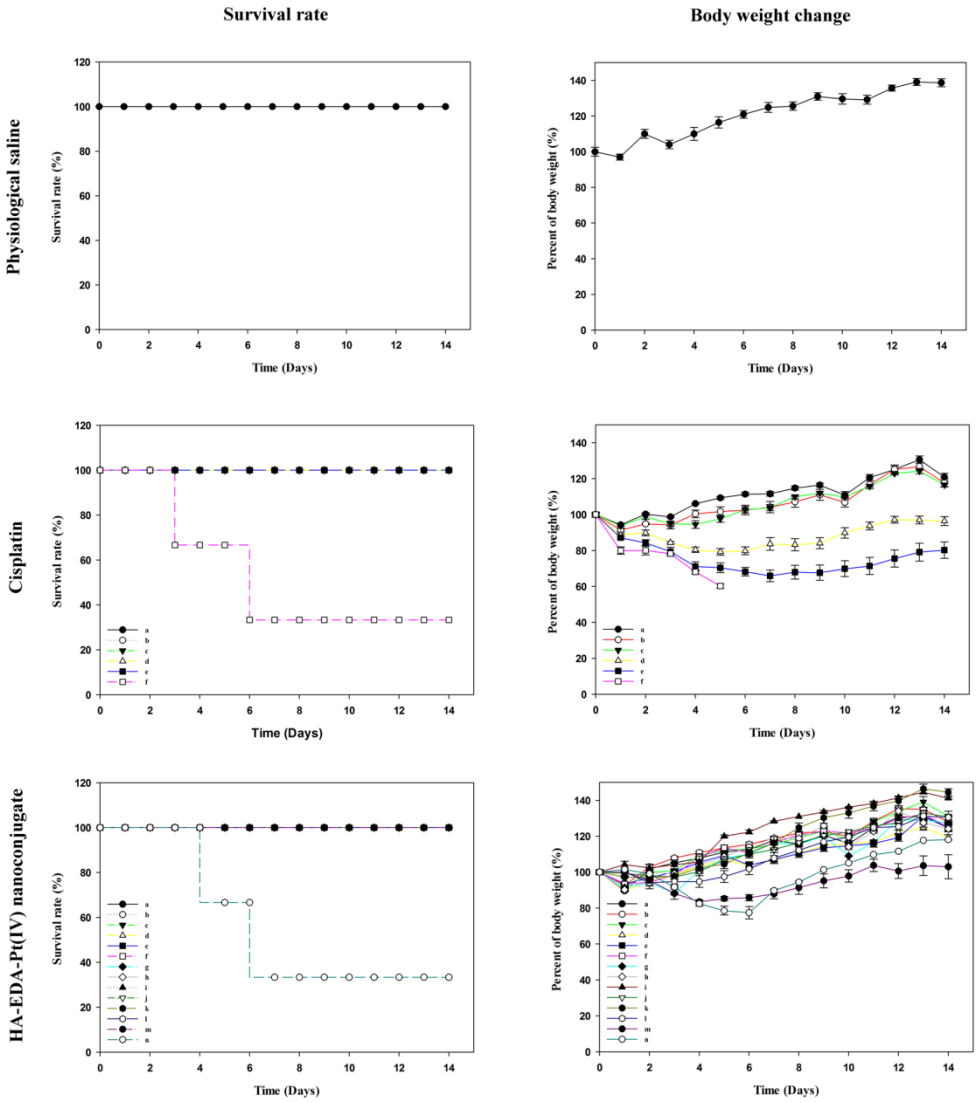

Fig. 4 Survival rate and body weight change of ICR mice treated with physiological saline; cisplatin at doses of (a) 3.375, (b) 4.500, (c) 6.000, (d) 8.000, (e) 10.670 and (f) 14.220 mg/kg; HA-EDA-Pt(IV) nanoconjugate at doses of (a) 25.816, (b) 34.421, (c) 45.894, (d) 61.192, (e) 81.590, (f) 108.787, (g) 145.049, (h) 193.398, (i) 257.865, (j) 343.819, (k) 458.426, (l) 611.234, (m) 814.979 and (n) 1086.639 mg/kg for evaluation of MTD.

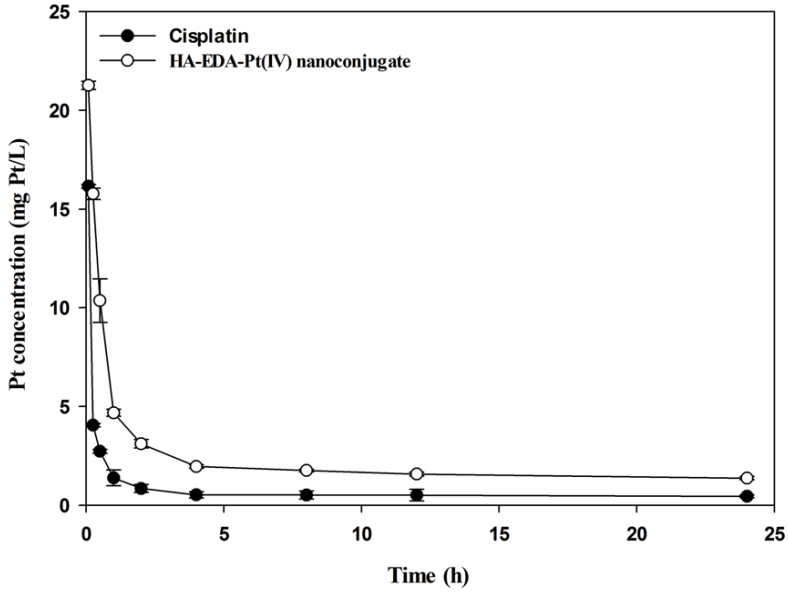

Fig. 5 *In vivo* pharmacokinetic curves of Pt concentration in the plasma versus time after a single intravenous injection of cisplatin and HA-EDA-Pt(IV) nanoconjugate in rats. Data were presented as means ± SD (n = 12).

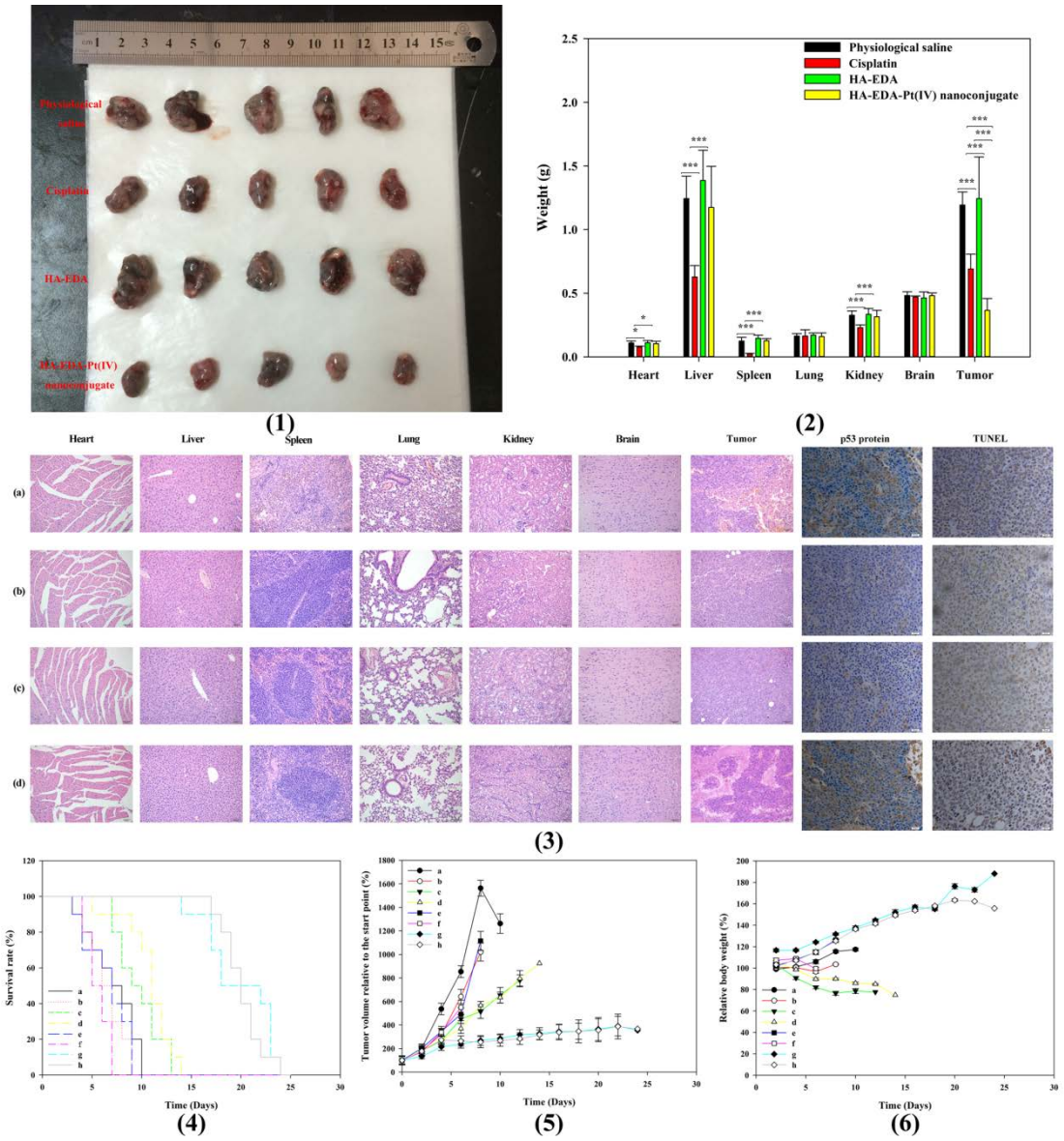

Fig. 6 (1) Comparison of tumor sizes from different groups, *i.e.*, physiological saline, cisplatin, HA-EDA and HA-EDA-Pt(IV) nanoconjugate; (2) Average weights of major organs (heart, liver, spleen, lung, kidney, brain) and tumors. Asterisk represented statistically significant differences compared to the respective physiological saline or HA-EDA controls (*, $p < 0.05$; **, $p < 0.01$; ***, $p < 0.001$); (3) *Ex vivo* histological observation for major organs and tumors with HE stain, tumor sections with immunohistochemistry and TUNEL; (a) cisplatin, (b) physiological saline, (c) HA-EDA, (d) HA-EDA-Pt(IV) nanoconjugate. Nuclei were stained bluish violet, and extracellular matrix and cytoplasm were stained pink in HE. Brown stains represented tumor protein p53 in immunohistochemistry. Brown stains indicated apoptotic cells in TUNEL; (4, 5 and 6) Survival, tumor size change and relative body weight change profiles of animals received corresponding treatments: physiological saline for (a) male and (b) female mice, cisplatin for (c) male and (d) female mice, HA-EDA for (e) male and (f) female mice, HA-EDA-Pt(IV) nanoconjugate for (g) male and (h) female mice.

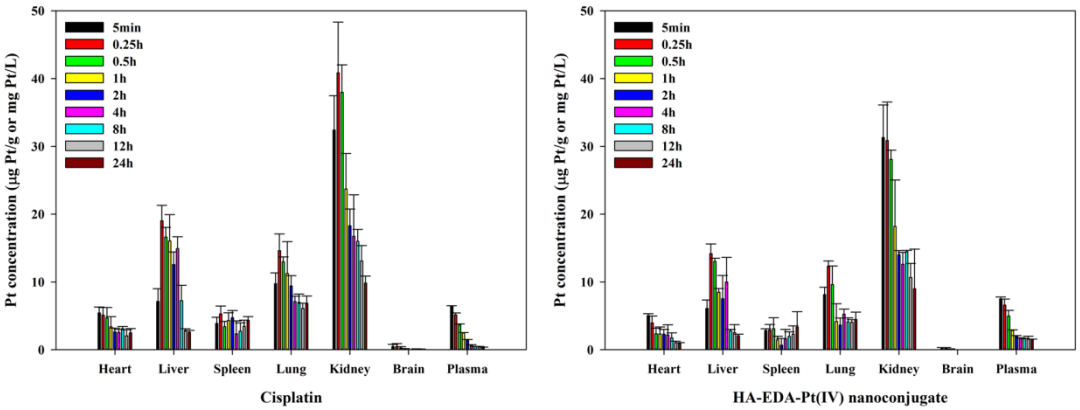

Fig. 7 Biodistribution of Pt concentration in heart, liver, spleen, lung, kidney brain and plasma at specified time points after an intravenous administration of cisplatin and HA-EDA-Pt(IV) nanoconjugate to normal mice. All date were normalized by weight of organs, that was, microgram per gram of respective organs, or volume of plasma, that was, milligram per liter of plasma, and expressed as averages ± SD from six animals per time point.

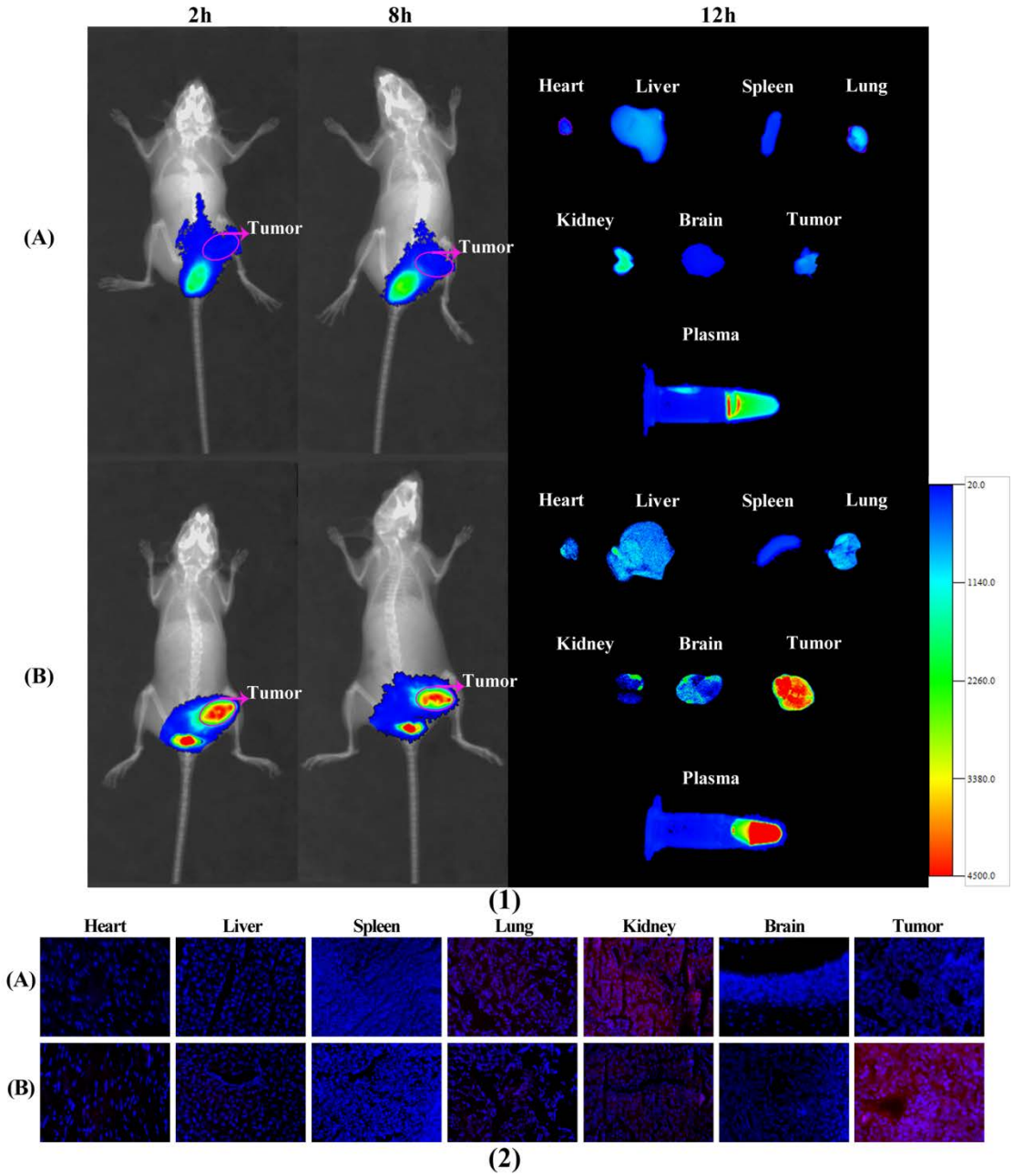

Fig. 8 Tumor-bearing mice were treated with (A) Cy7, SE (control) and (B) HA-EDA-Pt(IV)-Cy7, SE. (1) Specific targeting of the nanomedicine for HA receptor-overexpressed tumor was interpreted by fluorescent images acquired at 2 and 8 h and *ex vivo* fluorescent images of tumors, major organs and plasma collected after sacrificing the mice at 12 h. (2) Typical CLSM images of fluorescent signals (red) internalized by various tissues. The nuclei were stained with DAPI (blue).